A dynamically consistent dispersive gradient-enhanced continuum model

Harm Askes & Andrei V. Metrikine
Faculty of Civil Engineering and Geosciences, Delft University of Technology, The Netherlands

ABSTRACT: A higher-order continuum model is derived from a discrete medium. The discrete medium is constructed such that isotropy of the second-order continuum can be obtained. A new continualization method is applied in which the kinematic coupling between discrete and continuous variables is relaxed. As a result, not only higher-order stiffness terms but also higher-order inertia terms enter the continuum. The dispersive behavior of the model is set by an internal length scale and an internal time scale. Energy considerations show that the model is unconditionally stable, in contrast to most other second-order models derived from a discrete medium. A comparison with other second-order models is given as well.

Keywords: higher-order continuum, dispersion, length scale, time scale, continualization.

1 INTRODUCTION

Several scales of observation exist in engineering and sciences, and in many applications they interact. Thus, multiple length scales may be relevant and must be taken into account. Since a detailed modeling on the lowest level of observation is normally not feasible, alternative strategies must be taken. For instance, homogenization or continualization approaches can be used to translate microscopic representations of materials into a homogeneous macroscopic continuum description.

In this paper, a continualization approach is taken in which a discrete medium (consisting of masses and springs) is translated into a continuum via Taylor series expansions. The truncation of the series determines how much information from the lower scale is included. So-called classical continua are obtained when the minimum number of terms in the series are incorporated, but these continua do not contain any material parameter that represents the micro-structural heterogeneity. Therefore, higher-order terms are included as well, and as a result the equations of motion include up to fourth-order derivatives of the displacements.

Below, a novel continualization procedure as developed in (Metrikine and Askes 2002) is used for a two-dimensional discrete medium. The strict kinematic coupling between discrete and continuous displacements (that is commonly employed in continualization procedures) is relaxed. Instead, a dimensionless weighting constant is introduced to account for the nonlocal interaction between the various particles of the discrete medium. In the resulting continuum equations the stiffness terms are always accompanied by inertia terms of the same order. Hence, the continuum is denoted as *dynamically consistent* (Metrikine and Askes 2002; Askes and Metrikine 2002). As a consequence of the dynamical consistency, not only an internal length scale but also an internal time scale enters the model. The dispersive behavior of the model is set by the internal length and time scales.

After the derivation of the equations of motion in Section 2, the stability of the model is confirmed in Section 3 via energy considerations as well as via a dispersion analysis. In both cases, a critical (minimum) value for the newly introduced weighting constant is determined. In Section 4, the comparison with other models from the literature is treated, and it is shown that the model developed here can be reduced to the other models via a specific selection of parameters. Section 5 demonstrates the presence of an internal time scale in the constitutive relations and in Section 6 some closing remarks are given.

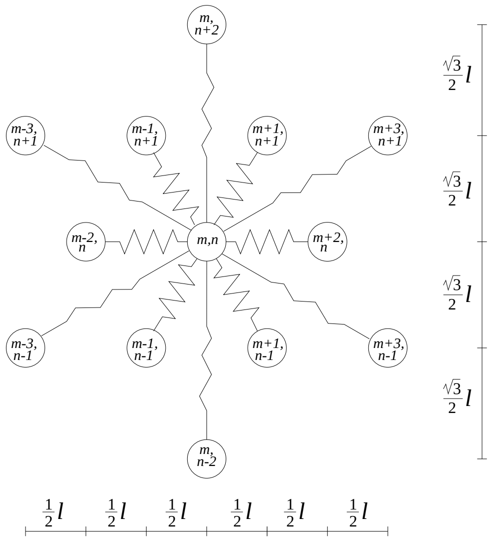

Figure 1: Extended hexagonal lattice

2 DERIVATION OF EQUATIONS OF MOTION

Various discrete representations of the material can be taken as the starting point of the continualization procedure. Furthermore, different types of interparticle contact (normal, transversal, rotational) can be accounted for (Suiker, de Borst, and Chang 2001; Suiker, Metrikine, and de Borst 2001). Below, the restriction is made to normal contact, which is represented by longitudinal springs between the particles. A hexagonal lattice has the advantage that the resulting classical continuum is isotropic without further assumptions. However, the corresponding second-order continuum is not isotropic, therefore the extended hexagonal lattice as depicted in Figure 1 is considered.

2.1 *Equations of motion of the discrete medium*

All particles depicted in Figure 1 are assumed to have the same mass M. The stiffness of the inner and outer ring of springs is denoted by K_1 and K_2, respectively. Then, the equations of motion can be written as

$$\begin{aligned} Mx^{(m,n)}_{,tt} &= \frac{K_1}{4}\Big\{-12x^{(m,n)}+4x^{(m+2,n)} \\ &+4x^{(m-2,n)}+x^{(m+1,n+1)}+x^{(m-1,n+1)} \\ &+x^{(m-1,n-1)}+x^{(m+1,n-1)}+\sqrt{3}\Big(y^{(m+1,n+1)} \\ &-y^{(m-1,n+1)}+y^{(m-1,n-1)}-y^{(m+1,n-1)}\Big)\Big\}+ \\ &\frac{K_2}{4}\Big\{-12x^{(m,n)}+3\Big(x^{(m+3,n+1)}+x^{(m-3,n+1)} \\ &+x^{(m-3,n-1)}+x^{(m+3,n-1)}\Big)+\sqrt{3}\Big(y^{(m+3,n+1)} \\ &-y^{(m-3,n+1)}+y^{(m-3,n-1)}-y^{(m+3,n-1)}\Big)\Big\} \end{aligned} \tag{1}$$

for the x-direction and

$$\begin{aligned} My^{(m,n)}_{,tt} &= \frac{K_1}{4}\Big\{-12y^{(m,n)}+3\Big(y^{(m+1,n+1)} \\ &+y^{(m-1,n+1)}+y^{(m-1,n-1)}+y^{(m+1,n-1)}\Big) \\ &+\sqrt{3}\Big(x^{(m+1,n+1)}-x^{(m-1,n+1)} \\ &+x^{(m-1,n-1)}-x^{(m+1,n-1)}\Big)\Big\} \\ &+\frac{K_2}{4}\Big\{-12y^{(m,n)}+4y^{(m,n+2)}+4y^{(m,n-2)} \\ &+y^{(m+3,n+1)}+y^{(m-3,n+1)}+y^{(m-3,n-1)} \\ &+y^{(m+3,n-1)}+\sqrt{3}\Big(x^{(m+3,n+1)}-x^{(m-3,n+1)} \\ &+x^{(m-3,n-1)}-x^{(m+3,n-1)}\Big)\Big\} \end{aligned} \tag{2}$$

for the y-direction. A subscript variable following a comma denotes a derivative. It is emphasized that the response of the discrete lattice is inherently anisotropic.

2.2 *Continualization procedure*

Next, Equations (1) and (2) are continualized via assumed relations between the discrete degrees of freedom x and y and the continuum degrees of freedom u_x and u_y. These relations consist normally of one-to-one links between the two sets of variables at the central particle (m,n). However, as has been shown in (Askes, Suiker, and Sluys 2002; Metrikine and Askes 2002; Askes and Metrikine 2002) this leads to higher-order gradient models of which the second-order truncation is unstable and of which the fourth-order truncation exhibits infinitely high velocities of waves and energy. Thus, this approach (refered to as the *standard continualization* approach) is intrinsically deficient, and alternative strategies must be pursued.

For a one-dimensional context a relaxed relation between the discrete and continuous degrees of freedom has been proposed in (Metrikine and Askes 2002). The one-to-one link at the central particle is dropped; instead, a weighted average is taken that also involves the neighboring particles. For the considered extended hexagonal lattice of Figure 1, this alternative continualization is written as

$$u_x = \frac{1}{1+6a_1+6a_2}\Big\{x^{(m,n)}$$

$$+\ a_1\Big(x^{(m+2,n)}+x^{(m+1,n+1)}+x^{(m-1,n+1)}$$

$$+\ x^{(m-2,n)}+x^{(m-1,n-1)}+x^{(m+1,n-1)}\Big)$$

$$+\ a_2\Big(x^{(m+3,n+1)}+x^{(m,n+2)}+x^{(m-3,n+1)}$$

$$+\ x^{(m-3,n-1)}+x^{(m,n-2)}+x^{(m+3,n-1)}\Big)\Big\} \qquad (3)$$

for the x-direction, and

$$u_y = \frac{1}{1+6a_1+6a_2}\Big\{y^{(m,n)}$$

$$+\ a_1\Big(y^{(m+2,n)}+y^{(m+1,n+1)}+y^{(m-1,n+1)}$$

$$+\ y^{(m-2,n)}+y^{(m-1,n-1)}+y^{(m+1,n-1)}\Big)$$

$$+\ a_2\Big(y^{(m+3,n+1)}+y^{(m,n+2)}+y^{(m-3,n+1)}$$

$$+\ y^{(m-3,n-1)}+y^{(m,n-2)}+y^{(m+3,n-1)}\Big)\Big\} \qquad (4)$$

for the y-direction. These relations can be considered as an average whereby the inner ring of particles are weighted by a factor a_1 and the outer ring of particles by a factor a_2. The factor $(1+6a_1+6a_2)$ serves as a normalizing factor.

In the above Equations the continuum variables u_x and u_y are expressed in terms of the various discrete variables. However, when the discrete equations of motion are to be rewritten, the discrete variables have to be expressed in terms of u_x and u_y. To this end, u_x and u_y are developed in power series in terms of the inter-particle distance l, and Taylor series are used for the neighboring particles — see (Metrikine and Askes 2002) for a detailed discussion. With these amendments, the discrete equations of motion (1) and (2) can be transformed into equations of motion for a second-order continuum, i.e.

$$\rho u_{i,tt} - \frac{3}{2}A\rho l^2 u_{i,ttkk} = \frac{2}{5}E\left(u_{i,jj}+2u_{j,ij}\right) -$$

$$\frac{1}{40}El^2\left\{(24A-1)u_{i,jj}+(48A-4)u_{j,ij}\right\}_{,kk} \qquad (5)$$

where index notation has been used (i, j and k are indices related to the spatial directions x and y). Furthermore, $A=\frac{a_1+3a_2}{1+6a_1+6a_2}$, while ρ and E denote the classical mass density and Young's modulus, respectively. A few observations can be made with respect to the above Equation:

- Both the inertia contributions (in terms of ρ) and the stiffness contributions (in terms of E) consist of a classical part of order l^0 and a second-order part of order l^2. Thus, the inertia terms always appear one-to-one with the stiffness terms of the same order. Hence, this model is denoted as being dynamically consistent (Metrikine and Askes 2002; Askes and Metrikine 2002).
- The second-order parts can be written as the Laplacian of the classical parts.
- The Poisson's ratio that can be retrieved from the classical stiffness term equals $\nu=\frac{1}{4}$.
- The mass density ρ and the Young's modulus E are linked to the discrete parameters via $M=\rho l^2 h\sqrt{3}/2$ and $K_1=2Eh\sqrt{3}/5$, where h is the dimension in the third direction. With the requirement that $K_2=\frac{1}{9}K_1$, both the classical parts and the second-order parts of the equations of motion are isotropic.
- The standard continualization approach is retrieved by setting $A=0$. This would lead to a vanishing higher-order inertia contribution and a switched sign of the higher-order stiffness contribution.

3 STABILITY CONSIDERATIONS

The stability of the derived model can be verified via either an investigation of the energy functional or by means of a dispersion analysis. Both lead to certain requirements for the weighting parameter A.

3.1 Energy functional

The energy densities that correspond to the equations of motion derived above can be written in a quadratic form as

$$\mathscr{U}^{\mathrm{kin}} = \frac{1}{2}\rho\Big\{u_{x,t}^2+u_{y,t}^2$$

$$+\ \frac{3}{2}Al^2\left(u_{x,xt}^2+u_{x,yt}^2+u_{y,xt}^2+u_{y,yt}^2\right)\Big\} \qquad (6)$$

for the kinetic energy density, and

$$\mathscr{U}^{\text{pot}} = \frac{1}{5}E\Bigg\{(u_{x,x}+u_{y,y})^2+(u_{x,y}+u_{y,x})^2$$

$$+\,2u_{x,x}^2+2u_{y,y}^2+\frac{1}{16}l^2\Bigg[(48A-3)(u_{x,xx}^2+u_{y,yy}^2)$$

$$+\,u_{x,yy}^2+u_{y,xx}^2+(48A-2)(u_{x,xy}^2+u_{y,xy}^2)$$

$$+\,(48A-4)\Big((u_{x,xx}+u_{y,xy})^2+(u_{x,yy}+u_{y,xy})^2$$

$$+\,\,(u_{x,xy}+u_{y,xx})^2+(u_{x,xy}+u_{y,yy})^2\Big)\Bigg]\Bigg\} \qquad (7)$$

for the potential energy. Since all terms have been expressed as quadratic forms, it is easily seen that the kinetic energy is always positive definite. Also the classical contributions to the potential energy are always positive definite. However, restrictions on A should be applied for unconditional positive-definiteness of the higher-order contributions to the potential energy. In particular, the critical term in Equation (7) is preceded by $(48A-4)$, from which it follows that

$$48A-4\geq 0 \iff A\geq \tfrac{1}{12} \qquad (8)$$

3.2 Dispersion analysis

Alternatively, the propagation of harmonic waves can be analysed. The dispersive properties of the medium are set by the dependence of the phase velocity on the wave number, therefore this is equally known as dispersion analysis. For a wave that propagates in the direction set by α, with α the angle as measured from the x-axis, a plane harmonic wave is described by

$$u_x = \hat{A}_x \exp\{\mathrm{i}k\,(ct - x\cos\alpha - y\sin\alpha)\} \qquad (9)$$

and

$$u_y = \hat{A}_y \exp\{\mathrm{i}k\,(ct - x\cos\alpha - y\sin\alpha)\} \qquad (10)$$

where $\hat{A}_i$ is the amplitude in the i-direction, i is the imaginary unit, c is the phase velocity and k is the wave number. A compression wave is obtained by taking $\hat{A}_y=0$ with $\alpha=0$ or $\hat{A}_x=0$ with $\alpha=\frac{1}{2}\pi$. Conversely, a shear wave is simulated via $\hat{A}_x=0$ with $\alpha=0$ or via $\hat{A}_y=0$ with $\alpha=\frac{1}{2}\pi$.

When these values are substituted into Equation (5), for the compression wave it is found that

$$c_{\text{compr}}^2 = \frac{6E}{5\rho}\cdot\frac{\left(\frac{3}{2}A-\frac{5}{48}\right)(kl)^2+1}{\frac{3}{2}A\,(kl)^2+1} \qquad (11)$$

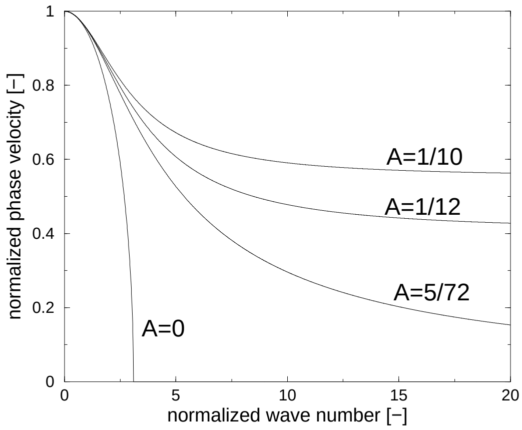

Figure 2: Dispersion curves: phase velocity versus wave number

and for the shear wave

$$c_{\text{shear}}^2 = \frac{2E}{5\rho}\cdot\frac{\left(\frac{3}{2}A-\frac{1}{16}\right)(kl)^2+1}{\frac{3}{2}A\,(kl)^2+1} \qquad (12)$$

Imaginary phase velocities may lead to instabilities, see for instance (Askes, Suiker, and Sluys 2002). For c^2 to be positive in the limit case $kl\to\infty$, the compression wave appears to be critical, from which it follows that

$$\tfrac{3}{2}A-\tfrac{5}{48}\geq 0 \iff A\geq\tfrac{5}{72} \qquad (13)$$

which yields a slightly lower value compared to Equation (8). This can be understood as follows: in the derivation of expression (8) it was required that every *individual* term of the energy functional is strictly non-negative, whereas in the dispersion analysis positiveness of a *conjunction* of contributions is required. Thus, in the dispersion analysis, certain destabilising terms are compensated by other stabilising terms, which leads to a lower critical value for A.

In Figure 2 dispersion curves are plotted for the compression wave. The phase velocity c (normalized with respect to the classical compression wave velocity $\sqrt{6E/5\rho}$) is plotted versus the wave number (normalized with respect to the inter-particle distance l). A range of values for A is taken, including the critical values derived via energy considerations, cf. Equation (8), and via dispersion analysis, cf. Equation (13). Also, the dispersion curve for $A=0$ is plotted, which is also obtained in the above-mentioned standard continualization approach. This value leads to imaginary phase velocities and, thus, instabilities for $kl\geq\sqrt{48/5}\approx 3.1$.

For sufficiently large values of A, the model of Equation (5) is unconditionally stable. Furthermore, the phase velocity is a monotonically *decreasing* function of the wave number. Thus, the high-frequency waves always travel slower than the low-frequency waves, and the phase velocity of the classical continuum is never exceeded. A horizontal asymptote is reached for $kl \to \infty$, the level of which is set by the value of A.

4 COMPARISON WITH OTHER MODELS

The stability of the model of Equation (5) becomes manifest through the different signs with which the classical and higher-order stiffness contributions enter the model. This bears resemblance to the gradient elasticity model proposed earlier by Aifantis and coworkers (Triantafyllidis and Aifantis 1986; Ru and Aifantis 1993; Altan and Aifantis 1997; Aifantis 1999; Gutkin and Aifantis 1999), which is normally written in the format of a constitutive relation as

$$\sigma_{ij} = D_{ijkl}\left(\varepsilon_{kl} - c\,\nabla^2\varepsilon_{kl}\right) \tag{14}$$

where σ and ε denote the stress and the strain, respectively, and D contains the linear elastic moduli. Furthermore, c is a (positive) constant with the dimension of length, which plays a role similar to that of l^2 in Equation (5). It has been proven in many occasions that the gradient term in Equation (14) can be used effectively to remove singularities from the strain field, see for instance (Aifantis 1999). However, since this model is formulated solely in terms of constitutive relations, higher-order inertia contributions are lacking. As a result, while the model of Equation (14) is unconditionally stable, infinitely high phase velocities occur which are unrealistic (Askes, Suiker, and Sluys 2002).

Higher-order inertia terms have been proposed earlier, either phenomenologically (Vardoulakis and Aifantis 1994) or by applying Padé approximations (Rubin, Rosenau, and Gottlieb 1995; Chen and Fish 2001; Andrianov, Awrejcewicz, and Barantsev 2003). In the latter methodology, higher-order stiffness terms can be replaced by higher-order inertia terms, e.g.

$$\begin{aligned}\rho u_{i,tt} &= (1+c\nabla^2)E\left(u_{i,jj}+2u_{j,ij}\right)\\ &\approx \frac{1}{1-c\nabla^2}\,E\left(u_{i,jj}+2u_{j,ij}\right)\end{aligned} \tag{15}$$

which yields

$$(1-c\nabla^2)\rho u_{i,tt} = E\left(u_{i,jj}+2u_{j,ij}\right) \tag{16}$$

However, the higher-order stiffness contributions have vanished in this approach. This would correspond to taking $A=\frac{5}{72}$ in Equation (11). Stability is guaranteed and the higher-order inertia ensures that the phase velocities remain bounded.

The model developed here and given in Equation (5) combines the advantages of higher-order stiffness with the advantages of higher-order inertia: unconditional stability, smoothing of strain singularities in statics and finite phase velocities in dynamics.

5 INTERNAL TIME SCALE

Expression (5) shows the equations of motion in terms of displacement derivatives. It is equally possible to express the equations of motion in terms of a divergence of a Cauchy stress tensor, e.g.

$$\rho u_{i,tt} = \sigma_{ji,j} \tag{17}$$

in which the Cauchy stresses σ_{ij} are defined as

$$\begin{aligned}\sigma_{xx} = \frac{2}{5}E\Bigg\{&3u_{x,x}+u_{y,y}-\frac{1}{16}l^2\Big[(72A-5)u_{x,xxx}\\ &+(36A-3)u_{y,xxy}+(48A-3)u_{x,xyy}\\ &+(12A-1)u_{y,yyy}\Big]+\frac{15\rho}{4E}Al^2u_{x,xtt}\Bigg\}\end{aligned} \tag{18}$$

$$\begin{aligned}\sigma_{xy} = \frac{2}{5}E\Bigg\{&u_{y,x}+u_{x,y}-\frac{1}{16}l^2\Big[(24A-1)u_{y,xxx}\\ &+(36A-3)u_{x,xxy}+(48A-3)u_{y,xyy}\\ &+(12A-1)u_{x,yyy}\Big]+\frac{15\rho}{4E}Al^2u_{y,xtt}\Bigg\}\end{aligned} \tag{19}$$

$$\begin{aligned}\sigma_{yx} = \frac{2}{5}E\Bigg\{&u_{x,y}+u_{y,x}-\frac{1}{16}l^2\Big[(12A-1)u_{y,xxx}\\ &+(48A-3)u_{x,xxy}+(36A-3)u_{y,xyy}\\ &+(24A-1)u_{x,yyy}\Big]+\frac{15\rho}{4E}Al^2u_{x,ytt}\Bigg\}\end{aligned} \tag{20}$$

$$\begin{aligned}\sigma_{yy} = \frac{2}{5}E\Bigg\{&u_{x,x}+3u_{y,y}-\frac{1}{16}l^2\Big[(12A-1)u_{x,xxx}\\ &+(48A-3)u_{y,xxy}+(36A-3)u_{x,xyy}\\ &+(72A-5)u_{y,yyy}\Big]+\frac{15\rho}{4E}Al^2u_{y,ytt}\Bigg\}\end{aligned} \tag{21}$$

Remark 1 The formal derivation of the standard stresses σ_{ij} and the higher-order stresses τ_{ijk} via the Hamilton-Ostrogradsky principle is not treated here — see (Metrikine and Askes 2002) for details on the one-dimensional case.

Remark 2 Note that symmetry of the stress tensor σ_{ij} is lost: $\sigma_{xy} \neq \sigma_{yx}$. However, this only holds for the contributions related to A. The difference $\sigma_{xy} - \sigma_{yx}$ has a contribution with time derivatives, which indicates an angular momentum.

In equivalence with Equation (14), the stresses are not only related to the strains (i.e. the first derivatives of the displacements), but also to the second gradients of the strains. However, in addition the stresses are related also to the second time derivatives of the strains. Whereas the second spatial strain gradients are preceded by an internal length scale squared (in terms of the inter-particle distance l and the weighting parameter A), the second time derivatives of the strains are preceded by an internal time scale ζ squared given by

$$\zeta^2 = \frac{15\rho l^2 A}{4E} \tag{22}$$

The dependence of the stresses on the second time derivative of the strains should *not* be understood as viscosity, since this latter property would be related to the *first* time derivative of the strains. Hence, the internal time scale ζ is not related to a relaxation time, but rather to the wave propagation characteristics of the high-frequency waves.

6 CLOSURE

In this study, a dispersive gradient elastiticy model has been derived within a two-dimensional context. The equations of motion have been derived from a discrete lattice representation of the material; hence, the macroscopic mechanical parameters can be related to the microstructural properties. A new continualization method has been applied in which the discrete degrees of freedom and the continuum displacements are linked in an averaged sense. To this end, a dimensionless weighting constant is introduced. The resulting equations of motion for the continuum are *dynamically consistent*: every inertia term is accompanied one-to-one by a corresponding stiffness term. Thus, not only higher-order stiffness terms but also higher-order inertia terms have appeared. These higher-order inertia terms are crucial for the stability of the model, as has been shown by energy considerations and by a dispersion analysis. Furthermore, the higher-order inertia terms guarantee that the phase and group velocities remain bounded.

In a next study, the stresses and boundary conditions (both classical and higher-order ones) will be derived by means of the Hamilton-Ostrogradsky principle. Moreover, an interpretation of the higher-order boundary conditions will be given.

7 REFERENCES

Aifantis, E.C. 1999. Gradient deformation models at nano, micro, and macro scales. *ASME Journal of Engineering Materials and Technology* 121, 189–202.

Altan, B.S. and Aifantis, E.C. 1997. On some aspects in the special theory of gradient elasticity. *Journal of the Mechanical Behavior of Materials* 8, 231–282.

Andrianov, I.V., Awrejcewicz, J., and Barantsev, R.G. 2003. Asymptotic approaches in mechanics: new parameters and procedures. *ASME Applied Mechanics Reviews* 56, 87–110.

Askes, H. and Metrikine, A.V. 2002. One-dimensional dynamically consistent gradient elasticity models derived from a discrete microstructure. Part 2: static and dynamic response. *European Journal of Mechanics A/Solids* 21, 573–588.

Askes, H., Suiker, A.S.J., and Sluys, L.J. 2002. A classification of higher-order strain gradient models —linear analysis. *Archive of Applied Mechanics* 72, 171–188.

Chen, W. and Fish, J. 2001. A dispersive model for wave propagation in periodic heterogeneous media based on homogenization with multiple spatial and temporal scales. *ASME Journal of Applied Mechanics* 68, 153–161.

Gutkin, M.Y. and Aifantis, E.C. 1999. Dislocations in the theory of gradient elasticity. *Scripta Materialia* 40, 559–566.

Metrikine, A.V. and Askes, H. 2002. One-dimensional dynamically consistent gradient elasticity models derived from a discrete microstructure. Part 1: generic formulation. *European Journal of Mechanics A/Solids* 21, 555–572.

Ru, C.Q. and Aifantis, E.C. 1993. A simple approach to solve boundary-value problems in gradient elasticity. *Acta Mechanica* 101, 59–68.

Rubin, M.B., Rosenau, P., and Gottlieb, O. 1995. Continuum model of dispersion caused by an inherent material characteristic length. *Journal of Applied Physics* 77, 4054–4063.

Suiker, A.S.J., de Borst, R., and Chang, C.S. 2001. Micromechanical modelling of granular material. Part 1: Derivation of a second-gradient micro-polar constitutive theory. *Acta Mechanica* 149, 161–180.

Suiker, A.S.J., Metrikine, A.V., and de Borst, R. 2001. Comparison of wave propagation characteristics of the Cosserat continuum and corresponding discrete lattice models. *International Journal of Solids and Structures* 38, 1563–1583.

Triantafyllidis, N. and Aifantis, E.C. 1986. A gradient approach to localization of deformation. I. Hyperelastic materials. *Journal of Elasticity* 16, 225–237.

Vardoulakis, I. and Aifantis, E.C. 1994. On the role of microstructure in the behavior of soils: effects of higher order gradients and internal inertia. *Mechanics of Materials* 18, 151–158.